

# On the Design and Manufacturing of Small Single Phase Induction Motors toward Super Premium Efficiency Standards

Ioannis D. Chasiotis, *Student Member, IEEE*, Yannis L. Karnavas, *Senior Member, IEEE*

**Abstract** -- The single-phase induction motors (SPIMs) are widely used in numerous household and industrial applications and a large number of them is produced every year. If their efficiency is enhanced beyond the ordinary ratings, significant energy savings would be achieved despite their low output power. The small SPIMs have been included in the latest industrial efficiency standards. However, the so far conducted research efforts have not provided a robust and acceptable - from economic and manufacturing point of view- design procedure aiming to meet this goal. Thus, the authors propose here a design methodology which guarantees both the SPIMs satisfactory starting performance and improved efficiency. The presented methodology has been applied to 1.0 HP SPIM. The derived results obtained through finite element analysis (FEA) are compared to the corresponding ones derived from other examined design approaches in order to highlight the effectiveness of the proposed methodology.

**Index Terms**--, electrical machine design and manufacturing, high performance, industrial standards, premium and super-premium efficiency, single phase induction motor.

## I. INTRODUCTION

THE energy crisis and the recent environmental concerns motivated many countries to revise the already adopted efficiency standards for electrical motors [1]. Mandatory regulations worldwide have been recently adopted aiming to accelerate the motor market transformation toward IE3 (premium-efficiency) and IE4 (super-premium efficiency) efficiency classes [2]. The International Electrotechnical Commission (IEC) published in March 2014 a new efficiency standard (i.e. IEC 60034-30-1) that incorporates both single-phase and three-phase induction motors with 2, 4, 6 and 8 poles [3], whose output power ranges from 120 W to 1000 kW. The corresponding standard authority in USA (i.e. the National Electrical Manufacturers Association (NEMA)) has published a relevant efficiency standard too. A wide scope of general-purpose electrical motors and also the small single-phase induction motors (SPIMs) are involved in this standard. The aforementioned regulations came into force in Jan. 2017 and consequently the commercial SPIMs efficiency ratings have to comply at least with the specifications of IE3 class from now on.

The SPIMs represent the mechanical power source backbone in various industrial and household applications [4], such as compressors, air conditioners, heating-circulating pumps, fans, centrifugal, sewing and washing

machines, etc. They are manufactured with an output power which ranges from sub-fractional up to few kilowatts and they are also available in many configurations, such as shaded pole, split-phase, capacitor-start/induction-run, capacitor-start/capacitor-run and capacitor-run SPIMs. The last mentioned topology exhibits: a) simple structure, b) low manufacturing cost, c) ruggedness, d) high power factor and e) lower starting current than the other SPIMs types [5].

On the other hand, the capacitor-run SPIMs starting torque and efficiency can be considered as low. Their starting to nominal torque ratio is usually equal to 0.3-0.7. Regarding efficiency, the ordinary ratings vary from 64% up to 78% for 1.0 HP SPIMs according to the data retrieved from the commercial catalogues of several manufacturers. Since they are mostly used in low power applications, their low efficiency has not been considered so far as an important disadvantage. However, millions of them are produced every year. Additionally, recent research studies revealed that the SPIMs efficiency enhancement can lead to significant savings in energy consumption [6].

Therefore, the development of SPIMs with improved efficiency is a topic of great interest. For this purpose, various motor's modeling, design, manufacturing and control aspects have been examined. At first, the researchers focused on the development of more accurate models and equivalent circuits toward the better estimation of SPIM's performance [7]. Next, they majority of the works paid attention to the determination of the optimal stator and rotor topology. This involves: a) investigations on the impact of several geometrical parameters on the SPIM operational features [8], [9], b) the examination of different rotor slot shapes along with numerous alternative configurations (e.g. open, semi-closed, closed, shallow or deep bars) [10]-[12] and c) the incorporation of artificial intelligent methods into the design process [13], [14].

Moreover, new materials and manufacturing techniques have been tested. For example, the copper rotors have replaced the aluminum ones [15], the die-cast processing has been established as the most cost-effective solution for the mass production of SPIMs squirrel-cages [16] and the perspective of using magnesium for the rotor bars has been examined in [17]. Furthermore, advanced electrical steels have been used for the stator and rotor cores construction of small SPIMs [18]. However, the cost of these materials remains prohibitive for low power applications. Additionally, numerous investigations have been conducted regarding to the optimal value and placement of the capacitor [19], [20]. Despite the fact that many of the previously described methods may lead to satisfactory efficiency

---

I. D. Chasiotis and Y. L. Karnavas are with the Electrical Machines Laboratory, Department of Electrical and Computer Engineering, Democritus University of Thrace, Xanthi, GR-67100, Hellas, (e-mail: ichasiot@ee.duth.gr, karnavas@ee.duth.gr).

improvement, only few of them are acceptable from manufacturing and economic point of view. This observation reinforces the "strong" opinion of plenty researchers which claim that the SPIMs can not comply with the new efficiency standards [21]. Nonetheless, in a previous authors' work [17] some directions were provided toward this direction. However, in that work the developed SPIMs with copper rotor failed to present adequate starting torque.

Taking the above into consideration, the authors present here an overall integrated and cost-effective design methodology for the development of capacitor-run SPIMs that exhibit: a) satisfactory starting capability and b) efficiency in accordance with the latest standards. At first, a sensitivity analysis is performed in order to highlight the impact of: a) rotor bar cross-sectional area, b) run-capacitor value and c) auxiliary to main winding turns ration on the SPIM's operational characteristics. Also, three different design methods are examined and applied to the case of 1.0 HP SPIM. Then, the post-processing analysis of the obtained results contributes to the extraction of useful conclusions. Based on these findings, the authors developed a new design methodology which reduces the problem's complexity and concludes to a premium-efficiency SPIM topology by performing only a small number of FEA simulations.

## II. SPECIFICATIONS OF THE SPIM UNDER STUDY

The capacitor-run SPIM under study is a 4-poles motor with 24 stator slot and 30 die-cast copper rotor bars. The geometrical representations of the considered stator and rotor topologies are depicted in Fig. 1. A semi-closed trapezoidal configuration has been adopted for the rotor slot. The specific topology is narrow at the top. This benefits the reduction of the starting current due to the impact of diffusion effects. Generally, it is a quite simple structure that is frequently selected by many SPIMs manufacturers. A small value has been chosen for the rotor slot opening ( $b_{r0}$ ). A sensitivity analysis regarding the specific parameter revealed that when this feature increases, both motor's starting and nominal performance are deteriorated. The motor's operational characteristics are summarized in Table I. All the adopted specifications and the applied constraints are in accordance with the latest international standards and industrial trends. The minimum efficiency that a 1.0 HP SPIM has to present for IE3 and IE4 class is equal to 82.5% and 85.7% respectively. This justifies the efficiency target that has been set in this work. For completeness purposes, it must be mentioned that the minimum efficiency values for IE1 (standard efficiency) and IE2 (high efficiency) are equal to 72.1% and 79.6% respectively. An efficiency lower than 72.1% will be characterized as IE0 (i.e. below efficiency standards) throughout the paper.

## III. MODIFIED CLASSICAL DESIGN METHODOLOGY

The classical SPIM design methodology involves several steps and many assumptions that have to be made by the designer. It is a well-known process for both engineers and manufacturers and it is analytically described in [22]. Thus, only its most important features will be discussed here. Also,

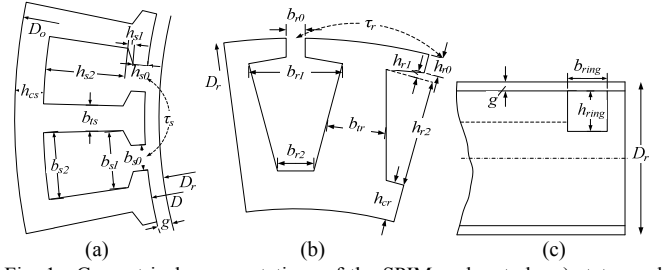


Fig. 1. Geometrical representations of the SPIM under study, a) stator and b) rotor slot topology and c) axial cross section of the rotor rings.

TABLE I  
SPIM UNDER STUDY CHARACTERISTICS

Parameter	Value
Rated output power, $P_n$	746 W
Rated output torque, $T_n$	$\geq 4.8$ Nm
Rated speed, $n_m$	$\geq 1420$ rpm
Line current (at 100% load), $I_n$	$\leq 5.0$
Efficiency (at 100% load), $\eta$	$> 82.5$ %
Power factor (at 100% load), $\cos\phi$	$\geq 0.9$
Starting to nominal torque ratio, $T_{st}/T_n$	$\geq 0.35$
Starting to nominal current ratio, $I_{st}/I_n$	$\leq 8.0$
Supply voltage, $U_n$	230 V
Rated frequency, $f$	50 Hz
Number of poles, $2p$	4
Motor's mass, $M$	$\leq 14.0$ kg

the authors' comments and their proposed modifications will be highlighted.

### A. SPIM Sizing

For given SPIM specifications, the product  $D_o^2 L$  (also known as utilization factor), is determined based on past experience. In this product,  $D_o$  is the motor's outer stator diameter and  $L$  is its axial effective length. The specific quantity is estimated by utilizing empirical curves (available in the literature), which represent the variation of  $D_o^2 L$  as a function of the SPIM's horsepower. Typical curves are illustrated in Fig. 2 for the case of small SPIMs and a variety of poles number ( $2p$ ).

Next, the inner stator diameter ( $D$ ) to  $D_o$  ratio is also empirically taken. This ratio usually varies from 0.5 to 0.75. In the case under study, its value has been set equal to 0.6. Then, the  $L/D$  ratio can be obtained from (1) ( $p$ : pole pairs). The  $L$  of the derived SPIM topologies will be smaller than  $D_o$  when this formula is adopted for  $2p$  equal or higher than 4.

$$L/D = \pi^3 \sqrt{p} / (2p) \quad (1)$$

Following the above, we obtain  $D_o^2 L = 2376.12$  cm<sup>3</sup>,  $D = 95.25$  mm,  $D_o = 157.86$  mm and  $L = 94.25$  mm. The calculation of stator slot geometrical characteristics (given in Fig. 1a), airgap length ( $g$ ) and rotor's outer diameter ( $D_r$ ) is conducted as described in [23].

### B. Squirrel-Cage Rotor Design

For the rotor slot design a starting point is needed. This is provided in Eq. (2), which correlates the bar slot cross-sectional area ( $A_{bar}$ ) with the corresponding one of the stator slot ( $A_s$ ). The stator ( $Q_s$ ) and rotor slots ( $Q_r$ ) number and the slot area factor ( $k_{bar}$ ) are also involved. A value between 0.35 and 0.6 is usually assigned to  $k_{bar}$ , as mentioned in [22]. When a high value is selected, the rotor slot becomes large.



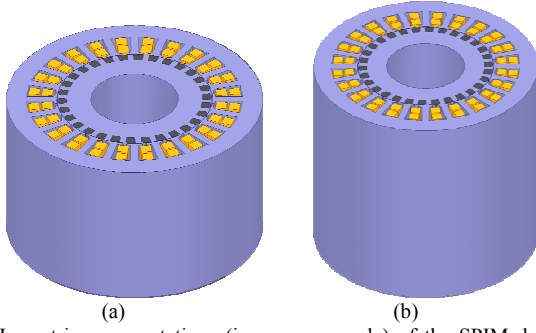


Fig. 4. Isometric representations (in common scale) of the SPIM designs derived from the three examined methods (related to  $D_o$  and  $L$ ): a) modified versions of classical design methodology (Method-A and Method-B) and b) alternative approach (Method-C).

frame.

c) Determine  $D_o^2 L$  by using the curves represented in Fig. 2 for given output power and poles number.

d) Calculate  $D_o$  for given  $L$  and afterwards calculate  $D$  by using  $D/D_o$  ratio (equal to 0.6) as mentioned in §III.A.

Following the above steps, we obtain: frame size: IEC 90L/NEMA 145T,  $D_o=137.87$  mm,  $D=83.41$  mm and  $L=125$  mm. The SPIM's length is now larger than the corresponding one derived from Method-A and Method-B. Geometrical representations of the two different SPIM designs are depicted in Fig. 4.

## V. EFFECT OF CRUCIAL DESIGN PARAMETERS

The impact of  $C_{run}$ ,  $k_{bar}$  and  $a$  on SPIM's operational characteristics is highlighted in this Section. By inspecting both Fig. 5 and further results (now shown here), we address and justify the main findings for each examined quantity.

### A. Efficiency

For all the investigated design methods the efficiency increases as a smaller rotor slot area is used. This can be justified by proceeding to loss decoupling. Specifically, when the rotor slot area becomes larger: a) the main and auxiliary winding copper losses increase extensively due to the higher line current, b) significant increment occurs for core losses due to the higher magnetic flux density at the rotor's teeth, c) the capacitor and mechanical losses present slight variation and d) the rotor copper losses decrease as the rotor cage resistance becomes lower.

The topologies derived from Method-A exhibit the lowest efficiency, which ranges from 70.6% to 78.2%. These ratings are almost equal to the ones found in commercial SPIMs. Moreover, for these topologies the efficiency decreases up to 4% as the  $C_{run}$  becomes higher for given  $k_{bar}$  due to the higher capacitor and stator losses. An efficiency higher than 82.5% and close to the super-premium one is achievable for  $k_{bar}=0.2$  when Method-B and Method-C are adopted. When the  $k_{bar}$  is equal to 0.35 (as suggested in [22]), the efficiency is slightly higher than the ordinary ratings. All the losses types, except from the rotor copper losses, decrease when the capacitance becomes higher. The efficiency is maximized for specific value of  $C_{run}$  for all the examined variation range of  $k_{bar}$ . Generally, this quantity is maximized when the  $C_{run}$  ranges from 25 uF up to 30 uF. However, this improvement is lower than 2% for a small rotor slot cross-sectional area.

### B. Power Factor

The decrement of  $k_{bar}$  with the simultaneous increment of  $C_{run}$  benefits substantially this characteristic. A slight variation has been observed for the case of Method-A, as the power factor varies from 0.68 to 0.82. Following the Method-B and Method-C the power factor acquires significantly higher values even for a low value of  $C_{run}$ . Indicatively, it is mentioned that for Method-C and  $k_{bar}=0.2$  the power factor ranges from 0.95 to 1 along with the capacitor value.

### C. Starting to Nominal Torque Ratio

All the examined models derived from Method-B and Method-C succeeded to fulfill the set starting torque requirement. This did not happen for the topologies obtained from the Method-A. In this case, the  $T_{st}$  increases as the rotor slot area becomes small and a high value is used for  $C_{run}$ . Thus, for  $k_{bar}$  equal or higher than 0.35 the  $T_{st}$  was found low regardless of the capacitor value. Only 49 of the 221 examined models exhibit  $T_{st}/T_n$  ratio at least equal to 0.35.

### D. Starting Current

The SPIM's starting current decreases significantly as the rotor bar slot cross-sectional area becomes smaller and a high value is assigned to  $C_{run}$ . A smaller variation is observed for the case of Method-A. The starting current of these topologies ranges from 42 A to 49 A and thus the corresponding applied constraint regarding  $I_{st}/I_n$  ratio is not met. Moreover, the configurations obtained from Method-B exhibit 16% up to 33% higher starting current than the corresponding ones of Method-C for given  $k_{bar}$  and  $C_{run}$ . It seems that the SPIM's axial effective length increment (applied in the case of Method-C) benefits also the starting performance.

### E. Auxiliary to Main Winding Turns Ratio

When a higher value is assigned to  $k_{bars}$ , a higher value has also to be adopted for the turns ratio aiming the motor to present adequate starting torque. This results to a larger number for the auxiliary turns, which increases extensively the stator copper losses and consequently deteriorates the efficiency. For  $k_{bar}=0.2$  (where the efficiency is maximized) the specific quantity ranges from 0.9 to 1.5. This variation range is quite different from the corresponding one proposed in [22]. Moreover, as the  $C_{run}$  increases the turns ratio decreases. Generally, the efficiency is maximized when this parameter is close to 1.0. Comparing the SPIM topologies derived from the Method-B and Method-C, a higher turns ratio value is always required for the former. In these cases, the used copper windings mass is larger which results to a higher manufacturing cost.

## VI. TOPOLOGIES COMPARISON AND DISCUSSION

A comprehensive comparison of the resulted SPIM topologies with the highest efficiency is conducted here. The SPIMs design and performance characteristics are summarized in Tables II and Table III for Method-B and Method-C respectively. Regarding these two design methods the followings are observed:



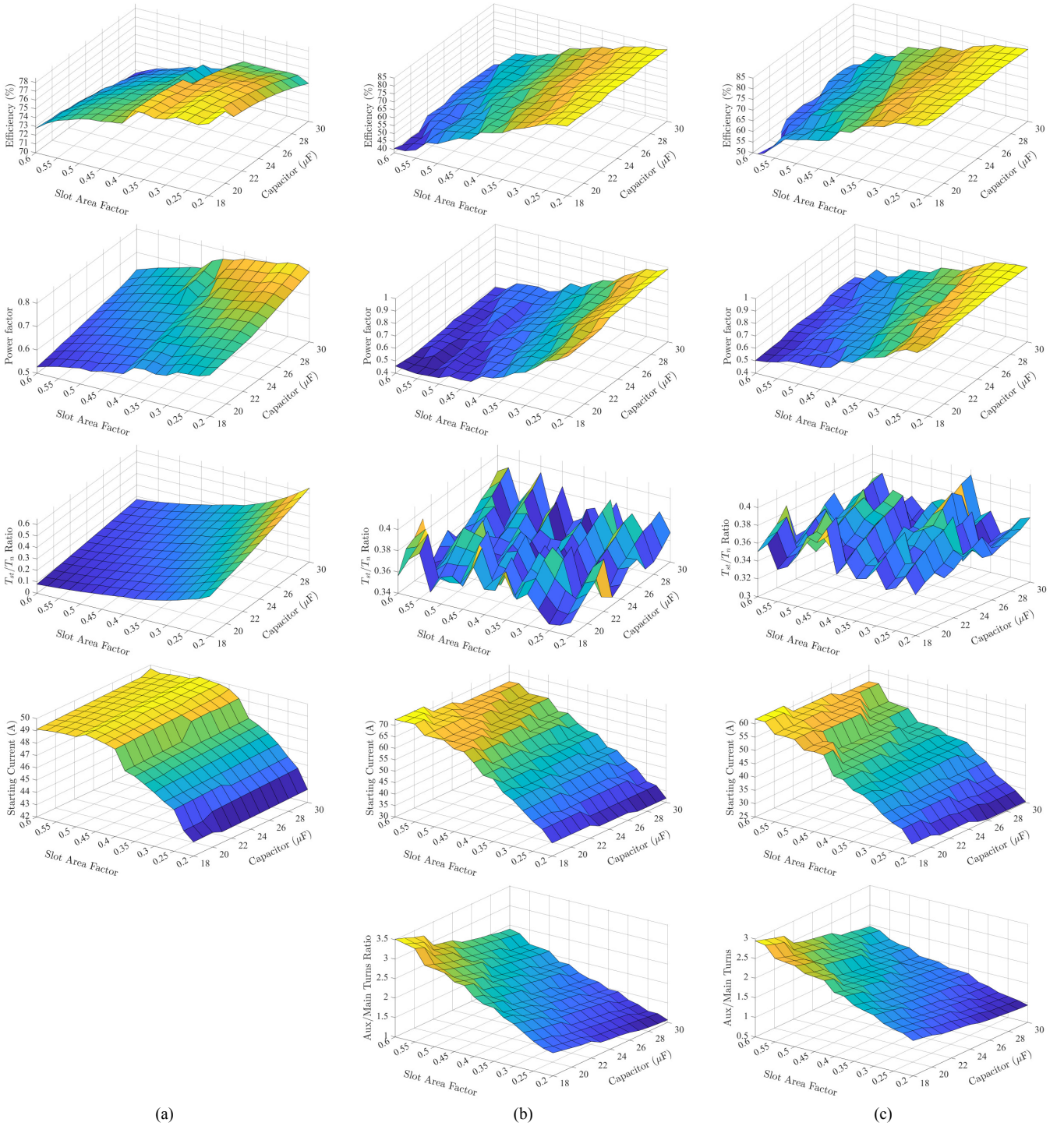


Fig. 5. Variation of efficiency, power factor, starting to nominal torque ratio, starting current and auxiliary to main winding turns ratio as a function of  $C_{run}$  and  $k_{bar}$  for the topologies derived from: a) Method-A, b) Method-B and c) Method-C. Is it noted that for Method-A the turns ratio value is constant and thus no variation is applied.

a) Method-C results to topologies with higher efficiency for all the examined variation range of  $k_{bar}$  (see Table IV). For  $k_{bar}=0.2$  the efficiency is higher by 0.37% up to 2.03%.

b) An efficiency higher than IE3 and slightly lower than IE4 is found for Method-C. The highest achievable efficiency (for  $C_{run}=26 \mu F$ ) is lower than the IE4 rating only by 1.61%. This is a strong evidence that the SPIMs efficiency can be significantly improved beyond the ordinary ratings and towards the latest industrial efficiency standards.

c) For Method-B the efficiency varies between IE3 and

IE4 for  $k_{bar}=0.2$  and  $C_{run}$  equal or higher than 23  $\mu F$ .

d) Method-C leads to SPIMs with superior performance for the majority of the examined load conditions according to the data given in Table V. It seems that important energy savings can be achieved when the SPIM operates at nominal and sub-nominal load conditions.

e) The masses of the SPIMs obtained from the Method-B are larger than the corresponding ones of Method-C by 0.82 kg up to 1.2 kg. Moreover, their manufacturing cost is higher by 12.4% up to 19.62%. The motors cost was calculated by

taking into account the materials consumption and their prices found in the international material market. The cost of the used run-capacitor was excluded.

f) When Method-B is followed, the core losses are higher by 13.3% up to 19.5%. For Method-C the core losses density varies from 4 to 4.5 W/kg. No magnetic saturation (Fig. 6) has been observed for the examined SPIM models.

g) Method-C results to SPIMs with lower starting current. The  $I_{st}/I_n$  ratio varies from 6.5 to 7.17 for Method-C. In the case of Method-B the specific ratio is almost equal to 8. In Fig. 7 the current density distribution under locked-rotor condition across the rotor slot's height and throughout its total cross-sectional area is depicted for two indicative topologies derived from the examined design methods.

## VII. PROPOSED SPIM DESIGN METHODOLOGY

Taking into consideration the obtained results (presented and commented in §V and §VI) and the extracted conclusions, the authors propose here an overall integrated design methodology for the development of capacitor-run SPIMs that exhibit both: a) satisfactory starting performance and b) efficiency at least equal or even higher than that imposed by IE3 efficiency class. As already demonstrated, the above can be achieved when  $N_m$  and  $a$  are properly selected. The presented methodology is organized in the followings steps:

**Step 1:** Specify the SPIM's characteristics and set the requirements and constraints for efficiency, starting torque starting current and main/auxiliary windings current density.

**Step 2:** Determine  $L$ ,  $D$  and  $D_o$  according to Method-C (as described in §IV).

**Step 3:** Select properly the  $Q_s/Q_r$  combination in order to avoid parasitic and undesirable phenomena.

**Step 4:** Set  $k_{bar}$  equal to 0.2 (it has been proven in the previous that a small rotor bar slot cross-sectional area benefits both SPIM's starting torque and efficiency).

**Step 5:** Calculate stator, rotor and end-ring geometrical parameters as described in §III.

**Step 6:** Set winding turns ratio ( $a$ ) equal to 1.5 and then obtain  $N_m$  and  $C_{run}$  from (8) and (10) respectively.

**Step 7:** Calculate  $N_a$  by using (9) and for given stator slot fill factor determine the wire diameter for the two windings.

**Step 8:** Create the SPIM model and perform FEA. If all the set requirements are met, the process stops here. Otherwise, continue with Step 9.

**Step 9:** If  $a$  is higher than 0.8, reduce its value by  $\Delta a$ , re-calculate the value of  $C_{run}$  and then go back to Step 7. If  $a < 0.8$ , continue with Step 10.

**Step 10:** Set  $a=1.5$ , increase  $N_m$  by  $\Delta N_m$ , re-calculate  $C_{run}$  and go back to Step 7. The process terminates when  $N_m$  cannot be further increased.

## VIII. CONCLUSIONS

In this work, it has been proven that the development of SPIMs with efficiency close enough to the super-premium ratings is feasible when the proposed here design methodology is adopted. To make this happen, the motor's axial length increment (with respect to frame size limits) is

TABLE II  
DESIGN PARAMETERS AND PERFORMANCE CHARACTERISTICS OF THE SPIM TOPOLOGIES DERIVED FROM **METHOD-B** FOR  $k_{bar}=0.2$

$C_{run}$ ( $\mu F$ )	$\eta$ (%)	$\cos\phi$	$a$	$N_a$	$N_m$	$I_{st}$ (A)	$I_{st}/I_n$	$M$ (kg)	$Cost$ (\\$)
18	81.72	0.885	1.592	624	392	35.68	7.96	13.13	49.32
19	81.97	0.889	1.541	604	392	35.64	8.01	13.21	49.76
20	81.83	0.894	1.500	588	392	35.60	8.02	13.07	48.97
21	81.69	0.897	1.449	568	392	35.55	8.03	12.99	48.53
22	81.50	0.906	1.429	560	392	35.54	8.09	12.96	48.35
23	83.06	0.944	1.290	516	400	33.39	8.06	12.78	47.28
24	82.94	0.948	1.260	504	400	33.35	8.07	12.76	47.17
25	82.78	0.954	1.240	496	400	33.32	8.12	12.70	46.86
26	82.70	0.957	1.200	480	400	33.26	8.09	12.64	46.51
27	83.52	0.976	1.127	460	408	31.92	8.02	12.57	46.13
28	83.43	0.977	1.098	448	408	31.86	7.99	12.53	45.88
29	83.30	0.981	1.078	440	408	31.82	8.02	12.50	45.71
30	83.16	0.984	1.059	432	408	31.79	8.04	12.47	45.54

TABLE III  
DESIGN PARAMETERS AND PERFORMANCE CHARACTERISTICS OF THE SPIM TOPOLOGIES DERIVED FROM **METHOD-C** FOR  $k_{bar}=0.2$

$C_{run}$ ( $\mu F$ )	$\eta$ (%)	$\cos\phi$	$a$	$N_a$	$N_m$	$I_{st}$ (A)	$I_{st}/I_n$	$M$ (kg)	$Cost$ (\\$)
18	83.02	0.951	1.400	504	360	29.46	7.17	12.14	43.35
19	82.94	0.956	1.356	488	360	29.43	7.18	12.08	43.03
20	82.82	0.958	1.311	472	360	29.39	7.18	12.03	42.72
21	83.31	0.978	1.228	452	368	27.91	7.01	11.94	42.24
22	83.53	0.980	1.196	440	368	27.87	7.03	11.80	42.01
23	83.43	0.983	1.163	428	368	27.84	7.04	11.86	41.78
24	83.35	0.985	1.130	416	368	27.80	7.03	11.82	41.55
25	83.68	0.995	1.053	400	380	26.18	6.73	11.78	41.29
26	84.09	0.999	1.021	392	384	25.42	6.58	11.74	41.11
27	84.01	0.999	1.000	384	384	25.39	6.56	11.72	40.96
28	83.93	1.000	0.969	372	384	25.35	6.55	11.68	40.77
29	83.84	1.000	0.948	364	384	25.31	6.54	11.65	40.59
30	83.76	1.000	0.938	360	384	25.28	6.52	11.64	40.52

TABLE IV  
EFFICIENCY RATINGS COMPARISON FOR THE SPIMs OBTAINED FROM **METHOD-B** AND **METHOD-C** AS A FUNCTION OF  $k_{bar}$  VALUE

$k_{bar}$	Method-B	Method-C
0.200	IE2-IE3 / IE3-IE4	IE3-IE4
0.225	IE2-IE3	IE2-IE3 / IE3-IE4
0.250	IE1-IE2 / IE2-IE3	IE2-IE3 / IE3
0.275	IE1-IE2 / IE2-IE3	IE2-IE3
0.300	IE1-IE2	IE1-IE3
0.325	IE1-IE2	IE1-IE2
0.350	IE1-IE2	IE1-IE2
0.375	IE1-IE2	IE1-IE2
0.400	IE0	IE1-IE2
0.425	IE0	IE1-IE2
0.45-0.6	IE0	IE0

TABLE V  
EFFICIENCY AND POWER FACTOR COMPARISON OF THE TOPOLOGIES FOR DIFFERENT LOAD CONDITIONS FOR  $C_{run}=18 \mu F$

Load Condition	Method-A $\eta$ (%)	Method-A $\cos\phi$	Method-B $\eta$ (%)	Method-B $\cos\phi$	Method-C $\eta$ (%)	Method-C $\cos\phi$
25 %	45.38	0.317	53.52	0.484	55.26	0.641
50 %	62.75	0.438	70.34	0.671	72.91	0.833
75 %	72.01	0.554	77.78	0.802	80.14	0.919
100 %	78.19	0.676	81.72	0.885	83.02	0.951
125 %	80.47	0.744	84.25	0.944	83.92	0.969
150 %	82.36	0.816	84.80	0.959	83.61	0.979

combined with the proper selection of crucial design parameters, such as the rotor cage topology and the windings characteristics. Useful directions are also provided for the determination of the above characteristics. The derived topologies were found to be preferable than the corresponding ones obtained through other design strategies presented up to now in literature, when various performance aspects were examined.

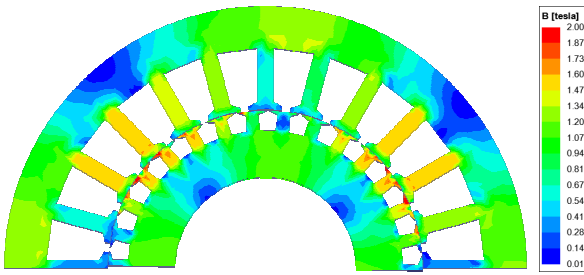


Fig. 6. View (1/2 part) and magnetic flux density distribution under rated performance of the SPIM with  $C_{mv}=18$  uF obtained from Method-C.

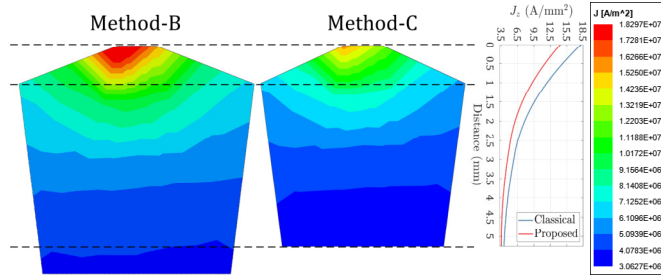


Fig. 7. Distribution of the rotor bar slot current density.

## IX. REFERENCES

- [1] C. J. Verucchi, C. R. Ruschetti, G. Kazlauskas, "High efficiency electric motors: economic and energy advantages", *IEEE Latin America Transactions*, vol. 11, issue 6, pp. 1325-1331, Dec. 2013.
- [2] F. J. T. E. Ferreira, Ge Baoming, A. T. de Almeida, "Reliability and operation of high-efficiency induction motors", *IEEE Transactions on Industry Applications*, vol. 52, issue 6, pp. 4628-4637, Nov. 2016.
- [3] L. Alberti, N. Bianchi, A. Boglietti, A. Cavagnino, "Core axial lengthening as effective solution to improve the induction motor efficiency classes", *IEEE Transactions on Industry Applications*, vol. 50, issue 1, 218-225, Jan.-Feb. 2014.
- [4] J. Malinowski, J. McCormick, K. Dunn, "Advances in construction techniques of ac induction motors preparation: for super-premium efficiency levels", *IEEE Transactions on Industry Applications*, vol. 40, issue. 6, pp. 1665-1670, 2004, doi:10.1109/TIA.2004.836300.
- [5] V. Sarac, N. Trajchevski, "Impact of capacitor on operating characteristics of single-phase motor", in *Proc. of 2019 6th Conf. on Electrical Machines, Drives and Power Systems (ELMA)*, Varna, Bulgaria, June 6-8, 2019.
- [6] D. Liang, V. Zhou, "Recent market and technical trends in copper rotor for high-efficiency induction motors", in *Proc. of 2018 International Power Electronic Conf. (IPEC-Niigata 2018- ECCE Asia)*, Niigata, Japan, May 20-24, 2018.
- [7] T. L. Lubin, S. Mezani, A. Rezzoug, "Analytical calculation of eddy currents in the slots of electrical machines: application to cage rotor induction motors", *IEEE Transactions on Magnetics*, vol. 47, no 11, pp. 4650-4659, Nov. 2011.
- [8] U. Sharma, B. Singh, "An approach to design of energy efficient single phase induction motor for ceiling fans", in *Proc. of 2019 IEEE International Electric Machines & Drives Conference (IEMDC)*, San Diego, USA, May 12-15, 2019.
- [9] E. B. Agamloh, A. Cavagnino, S. Vaschetto, "Impact of number of poles on the steady-state performance of induction motors", *IEEE Transactions on Industry Applications*, vol. 52, issue 2, pp. 1442-1430, Mar.-Ap. 2016.
- [10] S. Sobhani, H. Yaghoobi, M. Samakoosh, "Optimize efficiency and torque in the single-phase induction motor by adjusting the design parameters", in *Proc. of 12th International Conf. on Environment and Electrical Engineering*, Wroclaw, Poland, May 5-8, 2013.
- [11] G. Y. Zhou, J. X. Shen, "Current harmonics in induction machine with closed-slot rotor", *IEEE Transactions on Industry Applications*, vol. 53, issue 1, pp. 134-142, Jan. 2017.
- [12] H. J. Lee, S. H. Im, D. Y. Um, G. S. Park, "A design of rotor bar for improving starting torque by analyzing rotor bar resistance and reactance in squirrel cage induction motor", *IEEE Transactions on Magnetics*, vol. 54, issue 3, 2018.
- [13] D. Zhang, C. S. Park, C. S. Koh, "A new optimal design of rotor slot of three-phase squirrel cage induction motor for NEMA class D speed-torque characteristic using multi-objective optimization algorithm", *IEEE Transactions on Magnetics*, vol. 48, no. 2, pp. 879-882, Feb. 2012.
- [14] S. Wang, J. Kang, J. Noh, "Topology optimization of a single-phase induction motor for rotary compressor", *IEEE Transactions on Magnetics*, vol. 40, issue 3, pp. 1591-1596, May 2004.
- [15] W. R. Finley, M. M. Hodowanec, "Selection of copper versus aluminum rotors for induction motors", *IEEE Transactions on Industry Applications*, vol. 37, issue 6, pp. 1563-1573, Nov./Dec. 2001.
- [16] K. S. Lee, S. Ho Lee, J. H. Park, J. M. Kim, "Experimental and analytical study of single-phase squirrel-cage induction motor considering end-ring porosity rate", *IEEE Transactions on Magnetics*, vol. 53, issue 11, Nov. 2017.
- [17] Y. L. Karnavas, I. D. Chasiotis, "Design and manufacturing of a single-phase induction motor: A decision aid tool approach", *International Transactions on Electrical Energy Systems*, vol. 27, issue 9, e2357, Mar. 2017.
- [18] Z. Ling, L. Zhou, H. Li, W. Zhu, S. Guo, Jin Wang, "The use of electrical steels in single-phase induction machines and the modified iron loss test method", *IEEE Transactions on Magnetics*, vol. 50, issue. 11, Nov. 2014.
- [19] S. M. Hosseini, "Performance improvement of capacitor-run single-phase induction motor by non-orthogonal armature windings", in *Proc. of 2016 International Symposium on Power Electronics, Electrical Drives, Automation and Motion (SPEEDAM)*, Anacapri, Italy, June 22-24, pp. 1336-1341, 2016.
- [20] X. Wang, H. Zhong, Y. Yang, X. Mu, "Study of a novel energy efficient single-phase induction motor with three series-connected windings and two capacitors", *IEEE Transactions on Energy Conversion*, vol. 25, issue 2, pp. 433-440, June 2010.
- [21] D. G. Dorrell, "A review of the methods for improving the efficiency of drive motors to meet IE4 efficiency standards", *Journal on Power Electronics*, vol. 14, no. 5, pp. 842-851, Sept. 2014.
- [22] I. Boldea, S. A. Nasar, "The induction machines design handbook, 2nd edition", Boca Raton, FL, USA: CRC Press, 2010, ISBN: 9781420066685-CAT#66684.
- [23] J. Pyrhonen, T. Jokinen, V. Hrabovcova, "Design of rotating electrical machines, 2nd edition", West Sussex, UK: John Wiley & Sons Ltd., Nov. 2013, ISBN: 978-1-118-58757-5.

## X. BIOGRAPHIES

**Ioannis D. Chasiotis** was born in Athens, Hellas, 1991. He received the Diploma Degree in electrical and computer engineering from the Department of Electrical and Computer Engineering (DECE), Democritus University of Thrace (DUTH), Xanthi, Hellas. He is with the Electrical Machines Laboratory of the same Department and he is currently pursuing his Ph.D. degree.

His research interest are in the area of electrical machines design, the incorporation of optimization methods in the design process and the development of permanent magnet synchronous and inductions machines with characteristics of high power density and high efficiency. He has gained a full time award scholarship for his postgraduate studies from: a) Bodossaki Foundation (Sept. 2015-Aug. 2016) and b) Onassis Foundation (Oct. 2017-Feb. 2020).

He is member of the Hellenic Technical Chamber and student member of IEEE.

**Yannis L. Karnavas** (M' 98, SM' 19) was born in Volos, Hellas (Greece). He received the Diploma Degree and the PhD from the Department of Electrical and Computer Engineering (DECE), Democritus University of Thrace (DUTH), Xanthi, Hellas. He is with the Electrical Machines Laboratory of the DECE, DUTH.

His research interests include electrical machines design, analysis, modeling and optimization, controller design and application to electrical machines and artificial intelligence methods application to the above areas. He has published several papers in various international journals and conferences as well as book chapters in international engineering books. He has participated in many research projects as research leader or scientific associate. He serves as an Associate Editor and as an Editorial board member in various international scientific journals.

Prof. Karnavas is a chartered electrical engineer as well as a member of Hellenic Technical Chamber. Also, he is senior member of IEEE and member of PES, IAS and IES societies of IEEE.